NATIONAL ADVISORY COMMITTEE FOR AERONAUTICS

TECHNICAL NOTE 3759

ANALYSIS OF LAMINAR INCOMPRESSIBLE FLOW

IN SEMIPOROUS CHANNELS

By Patrick L. Donoughe

Lewis Flight Propulsion Laboratory
Cleveland, Ohio

NACA

Washington

August 1956

NATIONAL ADVISORY COMMITTEE FOR AERONAUTICS

TECHNICAL NOTE 3759

ANALYSIS OF LAMINAR INCOMPRESSIBLE FLOW IN SEMIPOROUS CHANNELS

By Patrick L. Donoughe

SUMMARY

Perturbation solutions of equations for laminar incompressible flow
in a semiporous channel are presented, and the results are compared with
those obtained from a fully porous channel. The perturbation parameter
measures the amount of suction or injection (blowing) at the porous
wall; positive values denote suction, and negative values denote blowing.

In the semiporous channel, with a given value of the perturbation
parameter, blowing decreased the friction parameter at the porous wall
by 25 percent, and suction increased the wall friction parameter by 50
percent. For both semiporous and fully porous channels, the pressure in
the longitudinal direction decreased for zero and blowing values of the
perturbation parameter. Sufficiently high suction values resulted in a
pressure rise in the fully porous channel. Either suction or blowing
has more influence on the local dimensionless velocity profiles and the
wall friction parameter for the semiporous than for the fully porous
channel.

INTRODUCTION

Experimental results for flow in a rectangular channel with injec-
tion through a porous wall are given in reference 1. Various porous
samples were installed in the lower wall; the upper wall was solid. In
the experiments, conducted with turbulent flow, the injection of air
through the porous wall markedly influenced the shape of the velocity
profile. The friction at the porous wall was obtained only qualita-
tively. The flow was developed with no injection, but not developed
when there was flow through the porous wall. Although additional tests
are indicated, it appears that some other geometry may be better suited
for the experimental investigation, and an analysis is needed to guide
the selection of the geometry. A significant turbulent-flow analysis
requires experimental data from the apparatus being sought, but laminar
flow may be treated theoretically. As part of the study to guide future
experiments, laminar flow in a semiporous channel is investigated here-
in. Results are compared with similar results in a fully porous channel.

Such an investigation has intrinsic value. Where the flow is re-
stricted by the proximity of bounding walls, it falls in the category of
either channel or pipe geometry. Such flow and geometry are found inside
bodies such as turbine blades and the skins of high-speed missiles whose
wall temperatures are reduced by the transpiration-cooling process.
Another application is for the equipment used in the separation of iso-
topes by the gaseous diffusion process. The present study should be of
interest in these applications.

Laminar flow in a channel with fully porous walls was studied ana-
lytically by Berman (ref. 2). Although only suction through the wall
was considered, results may be calculated readily for injection through
the wall. Before the publication of reference 2, Berman pointed out the
similarity between the flows in porous and semiporous channels (ref. 3).
The solution, however, was not given for the semiporous channel.
Berman's results for the fully porous channel, obtained by first-order
perturbation solutions and, therefore, valid for only small suction or
injection, are extended to large values of suction by Sellars (ref. 4).[1]

In the present investigation, a third-order perturbation solution
for laminar incompressible flow in a semiporous channel is presented.
Two-dimensional flow is considered. Velocity distributions, wall fric-
tion, and pressure drop are obtained from the solution for both suction
and blowing through the porous wall. A second-order perturbation solu-
tion is also obtained for the fully porous channel for comparison with
results from the semiporous channel.

SYMBOLS

A,B constants of integration (eqs. (12) and (A1))

f friction coefficient, $\mu\left(\dfrac{\partial u}{\partial y}\right)_w \bigg/ \dfrac{1}{2}\rho\bar{u}^2(x)$

g dimensionless stream function (eq. (6))

$g',g'',$ first, second, and third derivatives of g with respect to λ
g'''

---

[1] A different study of the flow in a fully porous channel with large
suction has been reported recently in an article by S. W. Yuan, entitled
"Further Investigation of Laminar Flow in Channels with Porous Walls."
Jour. Appl. Phys., vol. 27, no. 3, Mar. 1956, pp. 267-269.

h   channel height

p   static pressure

Δp_x pressure-change parameter in x-direction (eqs. (27) and (A7))

Δp_y pressure-change parameter in y-direction (eqs. (28) and (A8))

Re   main-flow Reynolds number, $2\bar{u}(x)h/\nu$

Re_0 main-flow Reynolds number, $2\bar{u}(0)h/\nu$

$Re_{w,fp}$ wall Reynolds number for fully porous channel, $v_w h/\nu$

$Re_{w,sp}$ wall Reynolds number for semiporous channel, $v_w h/2\nu$

$\bar{\bar{U}}$ velocity defined by eq. (7)

u   fluid velocity parallel to wall

v   fluid velocity normal to wall

W   channel width (fig. 1)

x   distance in main-flow direction

y   distance in normal flow direction

Γ nondimensional stream function for fully porous channel

$\Gamma', \Gamma'', \Gamma'''$ first, second, and third derivatives of Γ with respect to Λ

Λ nondimensional normal distance for fully porous channel, $2y/h$

λ nondimensional normal distance for semiporous channel, y/h

μ viscosity of fluid

ν kinematic viscosity of fluid, μ/ρ

ρ density of fluid

τ shear stress

Ψ stream function

Subscripts:

b   bottom wall

fp   fully porous channel

max   maximum

p   porous wall

s   solid wall

sp   semiporous channel

t   top wall

w   wall

x   x-direction

y   y-direction

Superscript:

—

            average values

ANALYSIS

Laminar-Flow Equations

A sketch of the geometry and flow system for the semiporous channel
is given in figure 1. The following development parallels that of
Berman (ref. 2). The channel width is assumed much greater than the
channel height; therefore, only two-dimensional flow need be considered.
The Navier-Stokes equations for two-dimensional steady-state incompres-
sible laminar flow neglecting body forces are (e.g., ref. 5, p. 48)

$$u\frac{\partial u}{\partial x} + v\frac{\partial u}{\partial y} = -\frac{1}{\rho}\frac{\partial p}{\partial x} + \nu\left(\frac{\partial^2 u}{\partial x^2} + \frac{\partial^2 u}{\partial y^2}\right) \tag{1}$$

$$u\frac{\partial v}{\partial x} + v\frac{\partial v}{\partial y} = -\frac{1}{\rho}\frac{\partial p}{\partial y} + \nu\left(\frac{\partial^2 v}{\partial x^2} + \frac{\partial^2 v}{\partial y^2}\right) \tag{2}$$

and the continuity equation is

$$\frac{\partial u}{\partial x} + \frac{\partial v}{\partial y} = 0 \tag{3}$$

The boundary conditions imposed on the system are

$$\left.\begin{array}{l} y = 0 \ (\text{solid wall}), \ u = 0; \ v = 0 \\[2mm] y = h \ (\text{porous wall}), \ u = 0; \ v = v_w = \text{constant} \end{array}\right\} \tag{4}$$

Transformation of Equations

The transformation of equations (1) and (2) is accomplished by the use of the substitutions

$$\lambda = \frac{y}{h} \tag{5}$$

and

$$g(\lambda) = \frac{\Psi}{h\left[\bar{u}(0) - \dfrac{v_w x}{h}\right]} = \frac{\Psi}{h\bar{U}} \tag{6}$$

where

$$\bar{U} \equiv \bar{u}(0) - \frac{v_w x}{h} \tag{7}$$

and $\bar{u}(0)$ is the average velocity at $x = 0$. Since $g = g(\lambda)$ only, the λ will be omitted hereafter.

The continuity equation (3) is satisfied by the stream function Ψ, since

$$\left.\begin{array}{l} u = \dfrac{1}{h}\dfrac{\partial\Psi}{\partial\lambda} = \bar{U}g' \\[4mm] v = -\dfrac{\partial\Psi}{\partial x} = v_w g \end{array}\right\} \tag{8}$$

and

Use of equations (1), (2), and (4) to (8) yields

$$-\frac{1}{\rho}\frac{\partial p}{\partial x} = \bar{U}\left[\frac{v_w}{h}(gg'' - g'^2) - \frac{\nu}{h^2}g'''\right] \tag{9}$$

and

$$-\frac{1}{\rho}\frac{\partial p}{\partial\lambda} = v_w\left(v_w gg' - \frac{\nu}{h}g''\right) \tag{10}$$

Since the right side of equation (10) is a function of λ only $(v_w = \text{constant})$,

$$\frac{\partial^2 p}{\partial \lambda \partial x} = 0 \tag{11}$$

Since $\bar{U} \neq 0$, on differentiating with respect to λ, using equation (11), and integrating, equation (9) becomes

$$Re_{w,sp}(g'^2 - gg'') + g''' = A \tag{12}$$

where

$$Re_{w,sp} \equiv \frac{v_w h}{\nu} \tag{13}$$

The boundary conditions (eqs. (4)) become

$$\left.\begin{array}{l} \lambda = 0 \text{ (solid wall), } g' = 0; \ g = 0 \\[2mm] \lambda = 1 \text{ (porous wall), } g' = 0; \ g = 1 \end{array}\right\} \tag{14}$$

Equations (12) to (14), in the present notation, are identical to those given in reference 3.

Solution of Equation

For small values of $Re_{w,sp}$, the perturbation solution of equation (12) is obtained by expanding g and A near $Re_{w,sp} = 0$:

$$g = g_0 + g_1 Re_{w,sp} + g_2 Re^2_{w,sp} + g_3 Re^3_{w,sp} + \cdots \tag{15}$$

$$A = A_0 + A_1 Re_{w,sp} + A_2 Re^2_{w,sp} + A_3 Re^3_{w,sp} + \cdots \tag{16}$$

Substituting equations (15) and (16) into equation (12) and equating like powers of $Re_{w,sp}$ yield

$$g_0''' = A_0 \tag{17}$$

$$g_1''' = A_1 + g_0 g_0'' - g_0'^2 \tag{18}$$

$$g_2''' = A_2 - 2g_0' g_1' + g_0 g_1'' + g_1 g_0'' \tag{19}$$

$$g_3''' = A_3 - 2g_0' g_2' + g_0 g_2'' + g_1 g_1'' + g_2 g_0'' - g_1'^2 \tag{20}$$

subject to boundary conditions

$$\left.\begin{array}{l} \text{for } \lambda = 0 \text{ (solid wall)}, \ g_n' = 0; \ g_n = 0 \\[2mm] \text{for } \lambda = 1 \text{ (porous wall)}, \ g_n' = 0; \ g_0 = 1, \ g_{n>0} = 0 \end{array}\right\} \quad (21)$$

Use of equations (15) to (21) yields the third-order solution of equation (12):

$$g = 3\lambda^2 - 2\lambda^3 + \frac{Re_{w,sp}}{70} \left(-16\lambda^2 + 27\lambda^3 - 21\lambda^5 + 14\lambda^6 - 4\lambda^7\right) +$$

$$\frac{Re_{w,sp}^2}{4,527,600} \left(-5,327\lambda^2 - 41,006\lambda^3 + 206,976\lambda^5 - 243,628\lambda^6 + \right.$$

$$99,792\lambda^7 - 24,255\lambda^8 + 21,560\lambda^9 - 17,248\lambda^{10} + 3,136\lambda^{11}\big) +$$

$$\frac{Re_{w,sp}^3}{1,765,764,000} \left(480,343\lambda^2 - 796,742\lambda^3 - 2,659,566\lambda^5 + 6,649,916\lambda^6 - \right.$$

$$4,666,740\lambda^7 + 2,162,160\lambda^8 - 2,902,900\lambda^9 + 3,107,104\lambda^{10} -$$

$$2,255,526\lambda^{11} + 1,729,455\lambda^{12} - 1,234,800\lambda^{13} + 446,880\lambda^{14} - 59,584\lambda^{15}\big)$$

$$(22)$$

and

$$A = -12 + \frac{81}{35} Re_{w,sp} - \frac{2,929}{53,900} Re_{w,sp}^2 - \frac{398,371}{147,147,000} Re_{w,sp}^3 \quad (23)$$

Absolute convergence of the series given by equations (22) and (23) has not been found. The perturbation solution, however, is compared with a numerical solution of equation (12) in the section Accuracy of Results.

Formulas for Velocity, Pressure, and Friction

The average velocity at an x location is given by

$$\overline{u}(x) = \int_0^1 u(x,\lambda) \ d\lambda$$

Use of equations (6) to (8), (13), and (14) shows that

$$\overline{U} = \overline{u}(x) = \overline{u}(0)\left[1 - \frac{v_w x}{\overline{u}(0)h}\right] = \overline{u}(0)\left(1 - \frac{2\mathrm{Re}_{w,sp}x}{\mathrm{Re}_0 h}\right) \qquad (24)$$

where

$$\mathrm{Re}_0 = \frac{2\overline{u}(0)h}{\nu}$$

Then, from equations (8), (24), and (22),

$$\left[\frac{u(x,\lambda)}{\overline{u}(x)}\right] = g' = 6(\lambda - \lambda^2) + \frac{\mathrm{Re}_{w,sp}}{70}(-32\lambda + 81\lambda^2 - 105\lambda^4 + 84\lambda^5 - 28\lambda^6) +$$

$$\frac{\mathrm{Re}_{w,sp}^2}{2,263,800}(-5,327\lambda - 61,509\lambda^2 + 517,440\lambda^4 - 730,884\lambda^5 +$$

$$349,272\lambda^6 - 97,020\lambda^7 + 97,020\lambda^8 - 86,240\lambda^9 + 17,248\lambda^{10}) +$$

$$\frac{\mathrm{Re}_{w,sp}^3}{1,765,764,000}(960,686\lambda - 2,390,226\lambda^2 - 13,297,830\lambda^4 +$$

$$39,899,496\lambda^5 - 32,667,180\lambda^6 + 17,297,280\lambda^7 - 26,126,100\lambda^8 +$$

$$31,071,040\lambda^9 - 24,810,786\lambda^{10} + 20,753,460\lambda^{11} - 16,052,400\lambda^{12} +$$

$$6,256,320\lambda^{13} - 893,760\lambda^{14}) \qquad (25)$$

The velocity ratio given in equation (25) is a function only of $\mathrm{Re}_{w,sp}$ and position λ but not position x. Thus, the flow may be considered to be developed.

Integrating $dp(x,\lambda) = \frac{\partial p}{\partial x}dx + \frac{\partial p}{\partial \lambda}d\lambda$ and using equations (9), (10), (12), (13), and (21) result in the pressure

$$p(x,\lambda) = p(0,0) + \frac{\mu A}{h^2}\overline{u}(0)x\left[1 - \frac{v_w x}{2\overline{u}(0)h}\right] + v_w\left(\frac{\mu}{h}g' - \frac{\rho v_w g^2}{2}\right) \qquad (26)$$

The pressure change in the x-direction may then be found from equations (26) and (23):

$$\Delta p_{x,sp} \equiv \frac{p(x,\lambda) - p(0,\lambda)}{\frac{1}{2}\rho\bar{u}^2(0)} = \frac{2x}{hRe_0}\left(-24 + \frac{162}{35}Re_{w,sp} - \frac{2,929}{26,950}Re^2_{w,sp} - \right.$$

$$\left. \frac{796,742}{147,147,000}Re^3_{w,sp}\right)\left(1 - \frac{Re_{w,sp}x}{Re_0 h}\right) \tag{27}$$

Note that λ does not appear on the right side of equation (27). This is a consequence of equation (11) and results from the assumption of a constant v_w. Similarly, the pressure change in the y-direction is

$$\Delta p_{y,sp} \equiv \frac{p(\lambda,x) - p(0,x)}{\frac{1}{2}\rho v_w^2} = \frac{p(\lambda,x) - p(0,x)}{\frac{1}{2}\rho\bar{u}^2(0)}\left(\frac{1}{2}\frac{Re_0}{Re_{w,sp}}\right)^2 = \frac{2g'}{Re_{w,sp}} - g^2 \tag{28}$$

The shear stress is given by

$$\tau_w = \mu\left(\frac{\partial u}{\partial y}\right)_w \tag{29}$$

and the friction coefficient may be defined as

$$f = \frac{\tau_w}{\frac{1}{2}\rho\bar{u}^2(x)} \tag{30}$$

Using equations (25), (29), and (30), the friction for the porous wall is obtained as

$$\frac{f_{sp,p}Re}{8} = \frac{-g''(1)}{2} = 3 + \frac{19}{70}Re_{w,sp} + \frac{124,033}{4,527,600}Re^2_{w,sp} + \frac{2,717,123}{1,765,764,000}Re^3_{w,sp} \tag{31}$$

(The negative sign appears because y increases as the porous wall is approached) and, for the solid wall, as

$$\frac{f_{sp,s}Re}{8} = \frac{g''(0)}{2} = 3 - \frac{8}{35}Re_{w,sp} - \frac{5,327}{4,527,600}Re^2_{w,sp} + \frac{480,343}{1,765,764,000}Re^3_{w,sp} \tag{32}$$

where $Re = 2\bar{u}(x)h/\nu$.

Accuracy of Results

In order to estimate the accuracy of the solution for the fully porous channel, the results from the perturbation solution are compared with the results from a numerical solution in table I. The comparison is made for $Re_{w,sp} = -4.0$.

Equation (12) was solved numerically by desk computation using the method of Picard (ref. 6, ch. XI). The characteristic values necessary for numerical integration of equation (12) are $g''(0)$ and A. The initial guesses for these values were taken from the perturbation solution. Successive trials finally gave the numerical results listed in table I. As is customary in problems of this type, $g''(0)$ and A must be obtained more accurately than g' for a given accuracy in g'.

Comparison of the numerical and perturbation solutions shows that $g''(0)$ from the third-order perturbation solution is accurate to within 0.13 percent, and $g''(1)$ is accurate to within 0.4 percent. (It is assumed that the numerical solution is correct.) This difference is expected from equations (31) and (32). A is accurate to within 0.008 percent. For values of $|Re_{w,sp}| < 4$, the third-order perturbation solution should be accurate to within 0.1 percent.

RESULTS AND DISCUSSION

The effects of flow through a porous wall are presented and discussed for semiporous and fully porous channels. The third-order solution for the semiporous channel is given in the ANALYSIS section; the second-order solution for a fully porous channel is given in the appendix. Some of the pertinent results of these solutions are listed in table II for different values of $Re_{w,sp}$.

Velocity Profiles

The local velocity ratio $u(x,\lambda)/\overline{u}(x)$ in the channel is shown in figure 2(a) for one porous and one solid wall, and for the fully porous channel. Both parts of the figure have $Re_{w,sp}$ as the parameter. For $Re_{w,sp} = 0 = Re_{w,fp}$, both curves are identical and the solutions of equations (12) and (A1) are exact.

Blowing (injection) occurs for $Re_{w,sp} < 0$ and is shown qualitatively in figure 1; suction occurs for $Re_{w,sp} > 0$. Positive values of $Re_{w,sp}$ place limits on $x/Re_0 h$. These limits are obtained by setting $\overline{u}(x) = 0$. Then, from equations (24) and (A6a), since $\overline{u}(0) \neq 0$,

$$\left(\frac{x}{Re_0 h}\right)_{max} = \frac{1}{2Re_{w,sp}} \tag{33}$$

for the semiporous channel, and

$$\left(\frac{x}{Re_0 h}\right)_{max} = \frac{1}{4Re_{w,sp}} \tag{34}$$

for the fully porous channel. For $|Re_{w,sp}| > 0$, there is a greater effect of $Re_{w,sp}$ on the local velocity ratio in the semiporous channel than in the fully porous channel. This may be seen by comparing both parts of figure 2(a).

Although $u/\overline{u}(x)$ is not a function of x, the velocity ratio $u/\overline{u}(0)$ is related to x. From equations (24) and (25),

$$\frac{u}{\overline{u}(0)} = \left(1 - \frac{2Re_{w,sp}x}{Re_0 h}\right)g' \tag{35}$$

and, from equations (A6),

$$\frac{u}{\overline{u}(0)} = \left(1 - \frac{4Re_{w,sp}x}{Re_0 h}\right)\Gamma' \tag{36}$$

These velocity ratios are given in figure 2(b) for $Re_{w,sp} = 0, 4,$ and -4 with the dimensionless distance $x/Re_0 h$ as parameter. The growth ($Re_{w,sp} = -4$) and retardation ($Re_{w,sp} = 4$) of the velocity ratio $u/\overline{u}(0)$ are evident. These velocity ratios are influenced more by wall Reynolds number in the fully porous channel than in the semiporous channel.

Note that, for a given value of $Re_{w,sp}$, the general shape of the curve is unchanged, even though the maximum values are different (fig. 2(b)). In a porous channel it is evident that fully developed flow defined by the velocity invariable with flow direction cannot be achieved. But, if fully developed flow is defined as a constant value of $u(x,\lambda)/\overline{u}(x)$ for increasing flow direction (with λ fixed), then there is obtained analytically fully developed flow in both the semiporous and fully porous channels when the suction Reynolds number is fixed (cf., eq. (25) and figs. 2(a) and (b)).

Pressure Distributions

The dimensionless pressure parameter in the y-direction Δp_y is presented in figure 3. These results are obtained by use of equations (28) and (A8). There is no pressure change across the channel when the

walls are solid ($v_w = 0$). In figure 3(a), when there is suction, the pressure parameter Δp_y (and hence $p(y,x)$) is higher than at the solid wall over most of the channel. For injection (blowing), the pressure in the channel is always less than at the solid wall. For either large suction or injection, $\Delta p_{y,sp}$ will always be less than at the solid wall. This may be seen by letting $Re_{w,sp} \to \infty$ in equation (28); since g^2 is always positive, $\Delta p_{y,sp}$ will be negative.

The pressure-change parameter $\Delta p_{y,fp}$ (fig. 3(b)) is referenced to the pressure at the center of the channel. Negative values of $Re_{w,sp} = 2Re_{w,fp}$ result in positive values of $\Delta p_{y,fp}$. Again it is found that, for either large suction or injection, the pressure parameter will be negative over the full channel, except at the center where it is zero. Such a solution is given by Sellars (ref. 4).

The results in figure 3 may be used to estimate the static-pressure drop across the channel. Equations (28) and (A8) may be expressed as

$$\frac{p(\lambda,x) - p(0,x)}{\frac{1}{2}\,\rho\bar{u}^2(0)} = \left(2\,\frac{Re_{w,sp}}{Re_0}\right)^2 \Delta p_y$$

where Δp_y is given in figure 3. Use of this equation and figure 3 shows that, when Δp_y is large, $Re_{w,sp}$ is small, and vice versa. Hence, for the usual value of $Re_{w,sp}/Re_0$ (say 0.01), the pressure change across the channel cross section should be small compared with the inlet dynamic head $\left(\frac{1}{2}\,\rho\bar{u}^2(0)\right)$. This pressure change is also small compared with the local dynamic head $\left(\frac{1}{2}\,\rho\bar{u}^2(x)\right)$ when there is blowing. With suction, however, the change may not be small compared with the local dynamic head, especially for large $x/Re_0 h$ (approaching $(x/Re_0 h)_{max}$).

The pressure-change parameter in the x-direction Δp_x is given in figure 4 for $0 \leq x/(Re_0 h) \leq 0.25$ and in figure 5 for $0 \leq x/(Re_0 h) \leq 0.035$. For both the semiporous and fully porous channels these figures indicate that Δp_x decreases for $Re_{w,sp} \leq 0$ (blowing). When $Re_{w,sp} > 0$, however, the analysis indicates a pressure rise $\Delta p_x > 0$ in the fully porous channel for sufficiently high values of $Re_{w,sp}$ (a similar result was noted in ref. 3). The same situation should obtain if solutions for higher values of $Re_{w,sp}$ are available for the semiporous channel. An explanation for this pressure rise may be as follows:

When solved for the pressure gradient, a momentum balance for a unit width of a channel yields

$$\frac{\partial p}{\partial x} = -\frac{1}{h}\left[(\tau_{w,t} + \tau_{w,b}) + \frac{\partial}{\partial x}\int_0^h \rho u^2 \, dy\right] \tag{37}$$

The wall shear stresses on the top and bottom walls are positive and of the same order of magnitude. When there is fluid injection, the momentum integral increases in flow direction; therefore, the pressure gradient decreases in flow direction. For the impermeable channel with fully developed flow, the momentum integral does not change in flow direction, so that the pressure gradient is still negative. With fluid suction, however, the integral term is negative. If the suction is sufficiently large, the integral term overcomes the shear terms and a pressure rise results $(\Delta p_x > 0)$.

Friction

The effects on the friction parameter of flow through the walls of a channel are presented in figure 6. The friction parameter is given for both the semiporous and fully porous channels for $-4 \leq Re_{w,sp} \leq 4$. The friction parameter at $Re_{w,sp} = 0$ is well established (ref. 7, p. 309; ref. 8, p. 51). Since there is a different boundary condition at each wall in equation (12), the effects of the flow through the wall are different at each wall of the semiporous channel. At the solid wall, blowing increases the friction parameter; at the porous wall, blowing decreases the friction parameter (fig. 6). The friction parameters at the porous wall for the semiporous channel for $Re_{w,sp} = 4$ and $Re_{w,sp} = -4$ are 50 percent above and 25 percent below, respectively, that of an impermeable wall. Corresponding numbers for the fully porous channel are 7 and 4.4 percent.

Although the friction parameter $fRe/8$ is not a function of x (e.g., eq. (31)), the friction coefficient f is related to x, since $Re = 2\bar{u}(x)h/\nu$. The average velocity $\bar{u}(x)$ is increased by blowing and decreased by suction. The effects of variations in the wall Reynolds number $Re_{w,sp}$, therefore, are greater on the friction coefficient f than on the friction parameter $fRe/8$.

SUMMARY OF RESULTS

Analytical solutions for incompressible laminar flow in a semiporous channel have been presented. A perturbation method was used to obtain the solutions. Results were compared with those for a fully porous channel. Some of the principal results are as follows:

1. Either suction or blowing is more influential on the wall friction parameter for the semiporous than for the fully porous channel. For wall Reynolds numbers of 4 and -4, the friction parameter at the porous wall of the semiporous channel is increased by 50 percent and decreased by 25 percent, respectively, from the value for impermeable channels.

In the semiporous channel, blowing diminishes the friction parameter at the porous wall and increases it at the solid wall; suction at the porous wall acts conversely. The friction coefficient behaves similarly.

2. The pressure in the longitudinal direction decreases for zero and for blowing values of the wall Reynolds number. This pressure drop occurs in both the semiporous and fully porous channels. A pressure increase was found for higher suction values in the fully porous channel and is indicated for the semiporous channel.

3. For both the semiporous and fully porous channels, the pressure change across the channel is small compared with the inlet dynamic head. Compared with the local dynamic head, the change is small for injection but may not be small for blowing at large values of the dimensionless distance x/Re_0h.

4. For a given value of the wall Reynolds number, the local velocity ratios are changed more in the semiporous than the fully porous channel. The velocity ratio built with inlet velocity acts conversely.

Lewis Flight Propulsion Laboratory
    National Advisory Committee for Aeronautics
        Cleveland, Ohio, April 25, 1956

APPENDIX - FORMULAS FOR A FULLY POROUS CHANNEL

Small Suction or Injection

The equation for a fully porous channel corresponding to equation (12) for a semiporous channel is given in reference 2 as, in the present notation,

$$\mathrm{Re}_{w,fp} \left(\Gamma'^2 - \Gamma\Gamma'' \right) + \Gamma''' = B \tag{A1}$$

where

$$\mathrm{Re}_{w,fp} = \frac{v_w h}{2\nu} = \frac{\mathrm{Re}_{w,sp}}{2}; \quad \Gamma = \Gamma(\Lambda), \quad \Lambda = 2y/h$$

y being measured now from midchannel (fig. 2(a)), since the flow is symmetrical about this plane. Boundary conditions are

$$\Lambda = 0 \quad \text{(midchannel)}, \quad \Gamma = 0; \ \Gamma'' = 0$$

$$\Lambda = 1 \quad \text{(porous wall)}, \quad \Gamma = 1; \ \Gamma' = 0$$

The zero- and first-order solutions from reference 2 are

$$\left.\begin{array}{l} \Gamma_0 = \dfrac{1}{2} \left(3\Lambda - \Lambda^3 \right) \\[2mm] \Gamma_1 = \dfrac{1}{280} \left(3\Lambda^3 - 2\Lambda - \Lambda^7 \right) \\[2mm] B_0 = -3 \\[2mm] B_1 = \dfrac{81}{35} \end{array}\right\} \tag{A2}$$

and the second-order equation is given as

$$\left.\begin{array}{l} \Gamma_2''' = B_2 + \Gamma_0\Gamma_1'' + \Gamma_1\Gamma_0'' - 2\Gamma_0'\Gamma_1' \\[4mm] \text{subject to} \\[2mm] \quad \Lambda = 0 \qquad \Gamma_2 = 0 = \Gamma_2'' \\[2mm] \quad \Lambda = 1 \qquad \Gamma_2 = 0 = \Gamma_2' \end{array}\right\} \tag{A3}$$

Integration of the equation for Γ_2''' and use of equation (A1) yield

$$\Gamma = \Gamma_0 + \Gamma_1 \, Re_{w,fp} + \Gamma_2 Re_{w,fp}^2 = \frac{1}{2}(3\Lambda - \Lambda^3) + \frac{Re_{w,fp}}{280}(3\Lambda^3 - 2\Lambda - \Lambda^7) +$$

$$\frac{Re_{w,fp}^2}{9,055,200}(-4,921\Lambda + 6,132\Lambda^3 + 1,386\Lambda^7 - 2,695\Lambda^9 + 98\Lambda^{11})$$

$$(A4)$$

$$B = B_0 + B_1 Re_{w,fp} + B_2 Re_{w,fp}^2 = -3 + \frac{81}{35} Re_{w,fp} - \frac{234}{13,475} Re_{w,fp}^2 \quad (A5)$$

From these relations, the velocity, pressure change, and friction may be obtained in the same manner as for the semiporous channel:

$$\frac{u}{\overline{u}(x)} = \Gamma' = \frac{3}{2}(1 - \Lambda^2) + \frac{Re_{w,fp}}{280}(9\Lambda^2 - 2 - 7\Lambda^6) +$$

$$\frac{Re_{w,fp}^2}{9,055,200}(-4,921 + 18,396\Lambda^2 + 9,702\Lambda^6 - 24,255\Lambda^8 + 1,078\Lambda^{10})$$

$$(A6)$$

where

$$\overline{u}(x) = \overline{u}(0)\left(1 - \frac{8Re_{w,fp}}{Re_0}\frac{x}{h}\right) \qquad (A6a)$$

$$\Delta p_{x,fp} = \frac{p(x,\lambda) - p(0,\lambda)}{\frac{1}{2}\rho\overline{u}^2(0)} = \frac{8B\nu x}{\overline{u}^2(0)h^2}\left[\overline{u}(0) - \frac{v_w x}{h}\right] = \left(\frac{x}{h}\frac{2}{Re_0}\right)\left(-24 + \frac{648}{35} Re_{w,fp} - \right.$$

$$\left. \frac{1,872}{13,475} Re_{w,fp}^2\right)\left(1 - 4\frac{Re_{w,fp}}{Re_0 h}x\right) \qquad (A7)$$

$$\Delta p_{y,fp} = \frac{p(\Lambda,x) - p(0,x)}{\frac{1}{2}\rho v_w^2} = \frac{p(\Lambda,x) - p(0,x)}{\frac{1}{2}\rho\overline{u}^2(0)}\left(\frac{Re_0}{4Re_{w,fp}}\right)^2 = \frac{2}{Re_{w,fp}}[\Gamma' - \Gamma'(0)] - \Gamma^2$$

$$(A8)$$

$$\frac{f_{fp} Re}{8} = -\Gamma''(1) = 3 + \frac{3}{35} Re_{w,fp} + \frac{5,516}{565,950} Re_{w,fp}^2 \qquad (A9)$$

REFERENCES

1. Eckert, E. R. G., Diaguila, Anthony J., and Donoughe, Patrick L.:
   Experiments on Turbulent Flow through Channels Having Porous Rough
   Surfaces with or without Air Injection. NACA TN 3339, 1955.

2. Berman, Abraham S.: Laminar Flow in Channels with Porous Walls.
   Jour. Appl. Phys., vol. 24, no. 9, Sept. 1953, pp. 1232-1235.

3. Berman, Abraham S.: Laminar Flow in Channels with Porous Walls.
   Rep. No. K-944., Carbide and Carbon Chem. Co., Oak Ridge (Tenn.),
   Nov. 28, 1952. (U.S. Govt. Contract W7405 eng 26.)

4. Sellars, John R.: Laminar Flow in Channels with Porous Walls at High
   Suction Reynolds Numbers. Jour. Appl. Phys., vol. 26, no. 4, Apr.
   1955, pp. 489-490.

5. Schlichting, Hermann: Boundary Layer Theory. McGraw-Hill Book Co.,
   Inc., 1955.

6. Scarborough, James B.: Numerical Mathematical Analysis. Second ed.,
   The Johns Hopkins Press (Baltimore), 1950.

7. Goldstein, S., ed.: Modern Developments in Fluid Dynamics. Vol. I.
   Clarendon Press (Oxford), 1938.

8. Kays, W. M., and London, A. L.: Compact Heat Exchangers. The Nat.
   Press, Palo Alto (Calif.), 1955.

CI-3

TABLE I. - COMPARISON OF PERTURBATION AND NUMERICAL

SOLUTIONS OF EQUATION (12) FOR $Re_{w,fp} = -4.0$.

Perturbation		Numerical (Picard's method)
7.756	$g''(0)$	7.747
-21.953	A	-21.955
-4.508	$g''(1)$	-4.525
0	$g(0)$	0
1.000	$g(1)$	1.000
g'	λ	g'
0	0	0
0.360	.05	.367
.667	.10	.671
1.125	.20	1.129
1.397	.30	1.400
1.509	.40	1.511
1.486	.50	1.488
1.351	.60	1.351
1.121	.70	1.120
.810	.80	.808
.431	.90	.431
.221	.95	.221
0	1.00	0

TABLE II. - VALUES FOR USE IN FRICTION AND

PRESSURE-CHANGE RELATIONS

Wall Reynolds number, $Re_{w,sp}$	Semiporous channel			Fully porous channel	
	$\dfrac{-g''(1)}{2}$	$\dfrac{g''(0)}{2}$	$-A$	$-\Gamma''(1)$	$-B$
4	4.623	2.084	3.786	3.210	-1.559
3	4.103	2.311	5.620	3.151	.432
2	3.665	2.540	7.610	3.095	.703
1	3.300	2.771	9.742	3.045	1.847
0	3	3	12	3	3
-1	2.755	3.227	14.37	2.960	4.161
-2	2.554	3.450	16.82	2.924	5.332
-3	2.391	3.668	19.36	2.893	6.510
-4	2.254	3.878	21.95	2.868	7.698
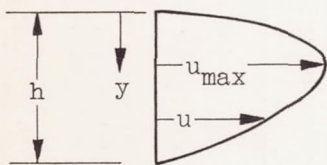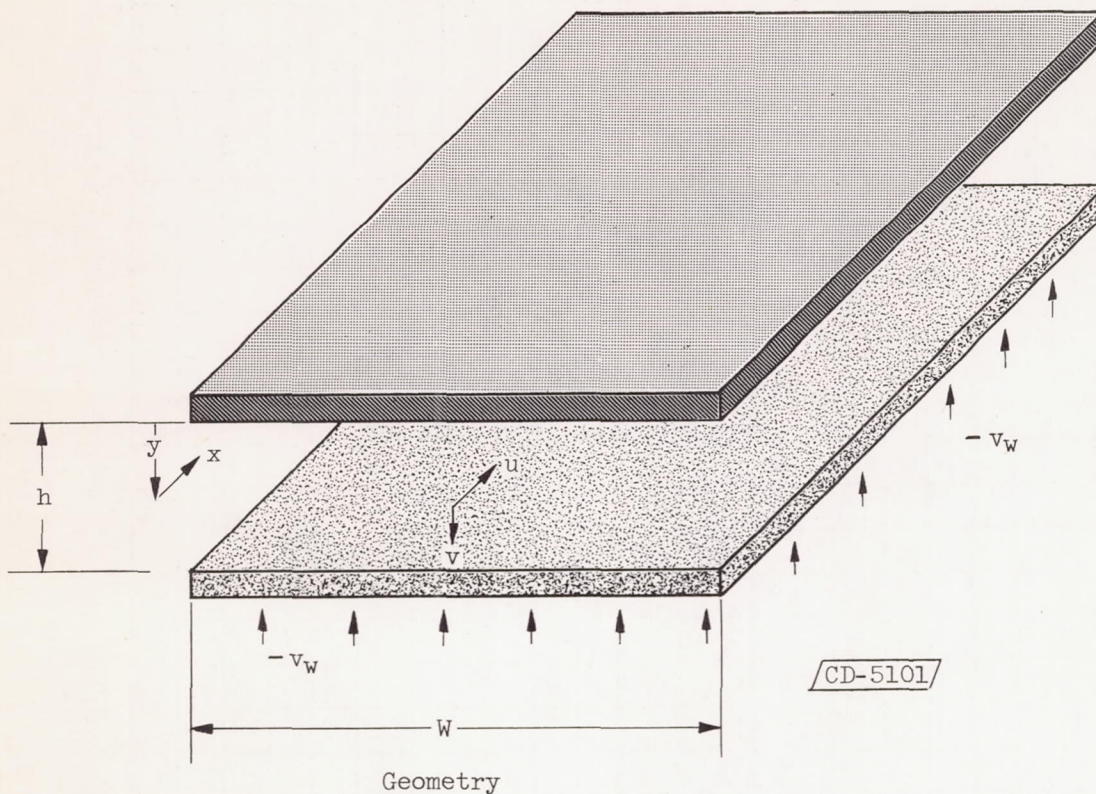
Geometry

$W >> h$
v_w = Constant
$\lambda = y/h$
$Re_{w,sp} = \dfrac{v_w h}{\nu}$

$+Re_{w,sp}$ (Suction)
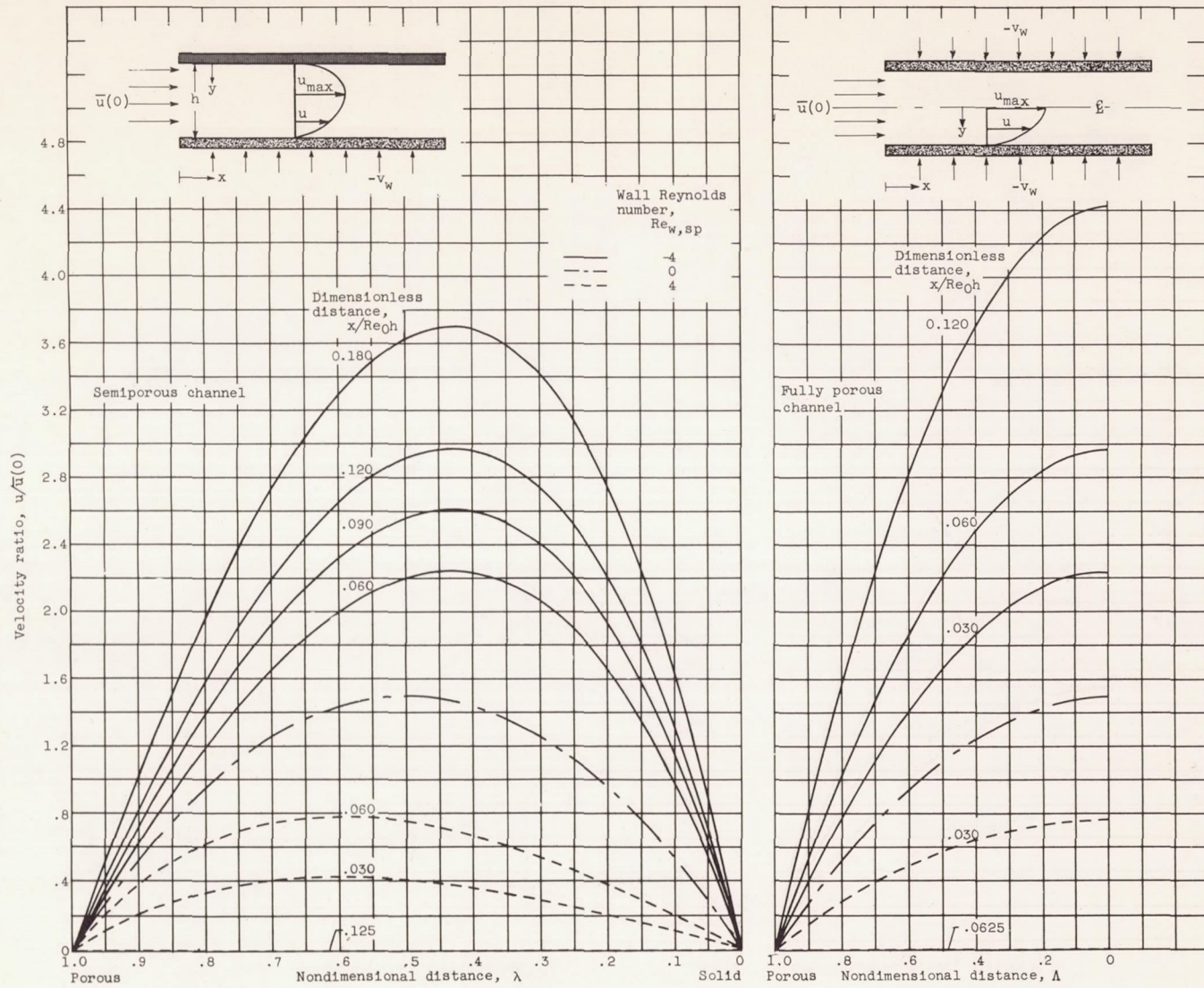$-Re_{w,sp}$ (Injection, depicted)

Velocity, $-Re_{w,sp}$

Figure 1. - Geometry and flow in semiporous channel.
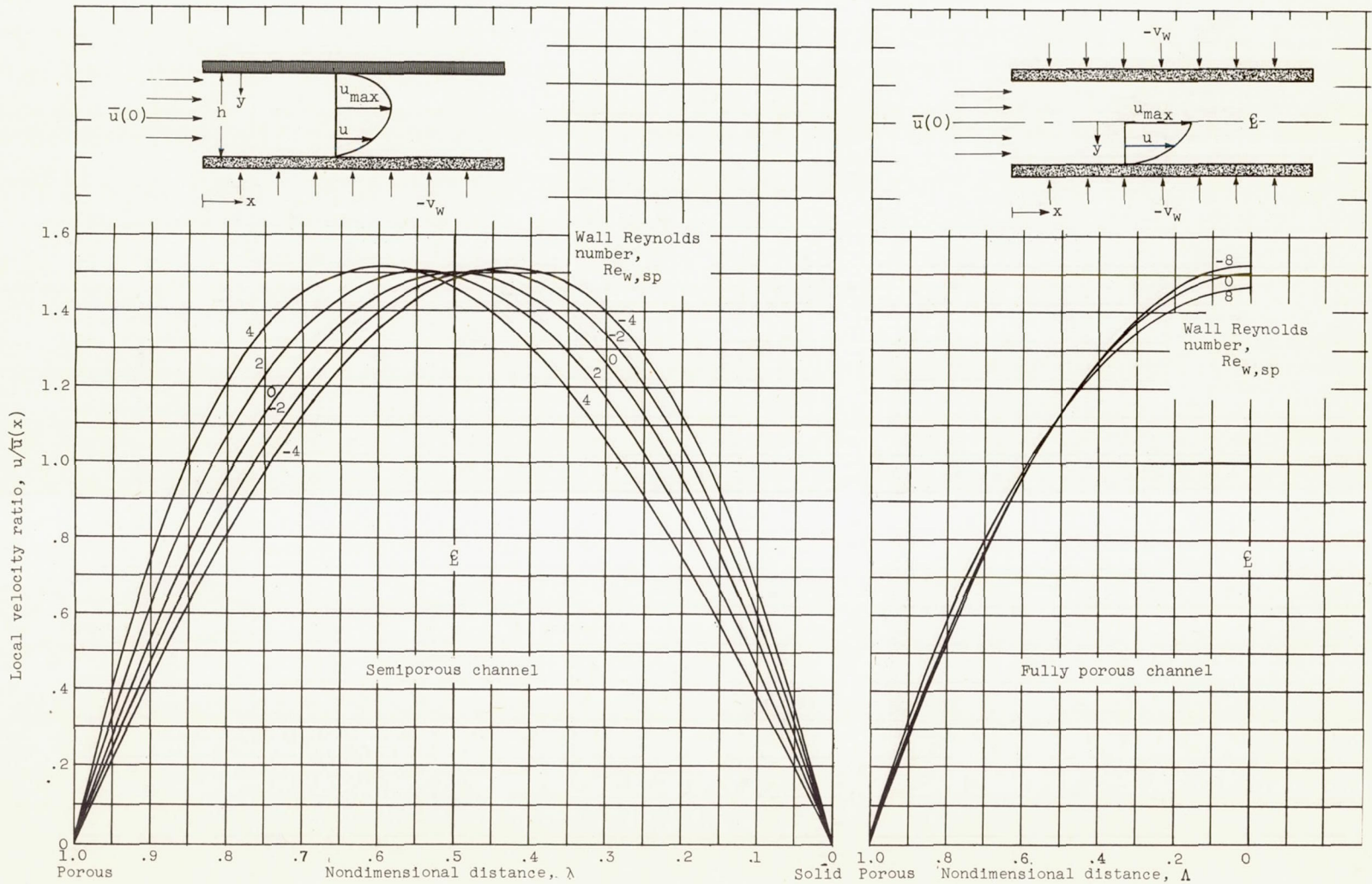
(a) Local velocity ratio.

Figure 2. - Velocity distribution in porous channels.

(b) Velocity ratio.

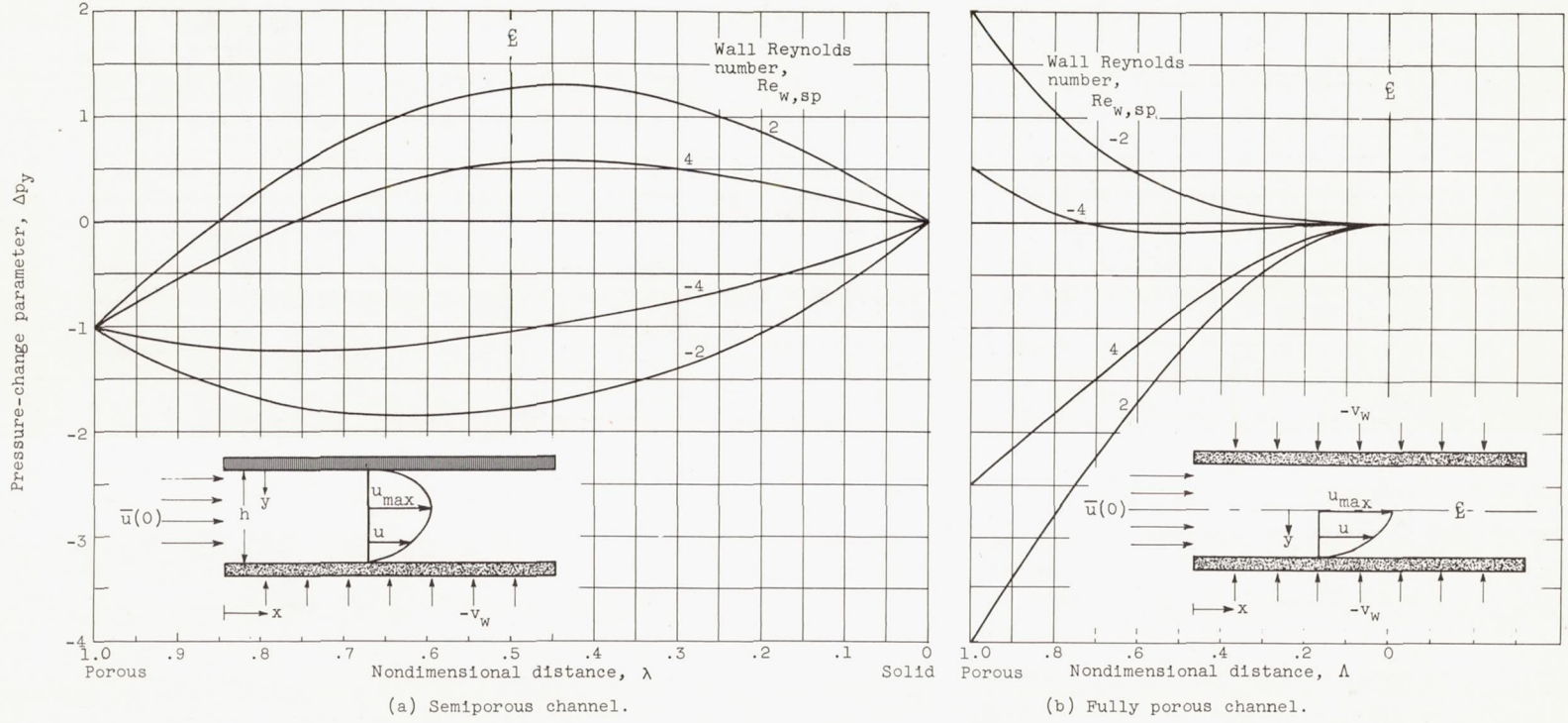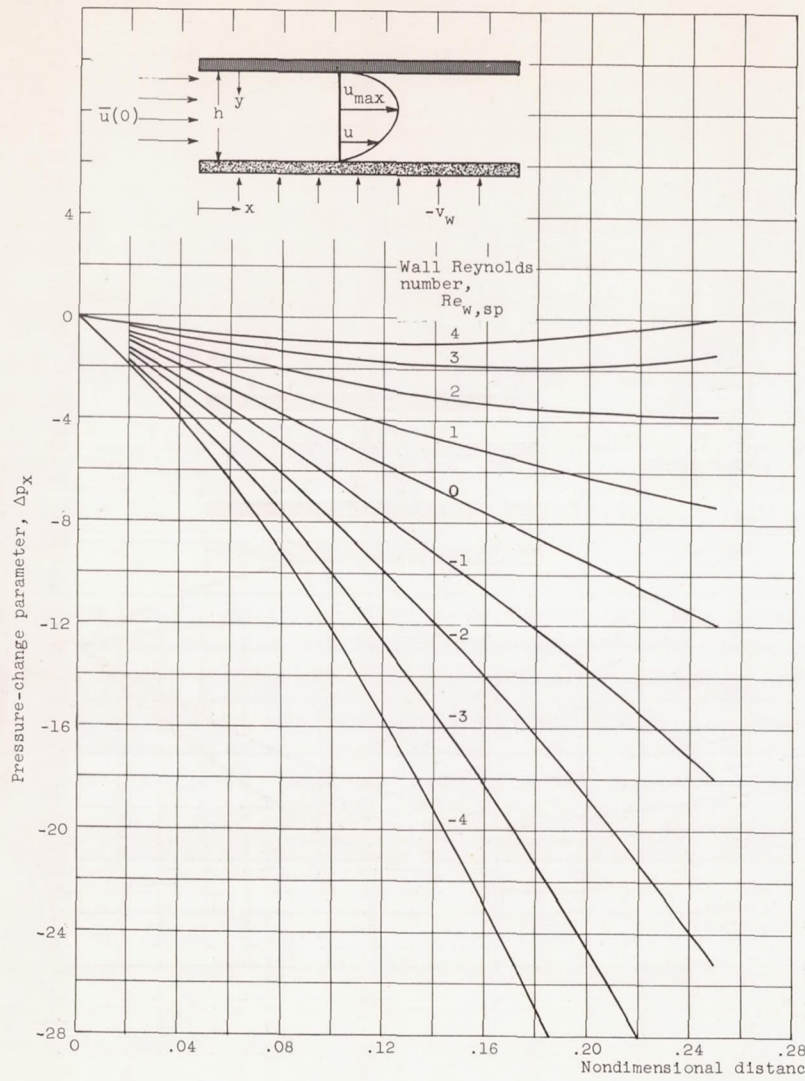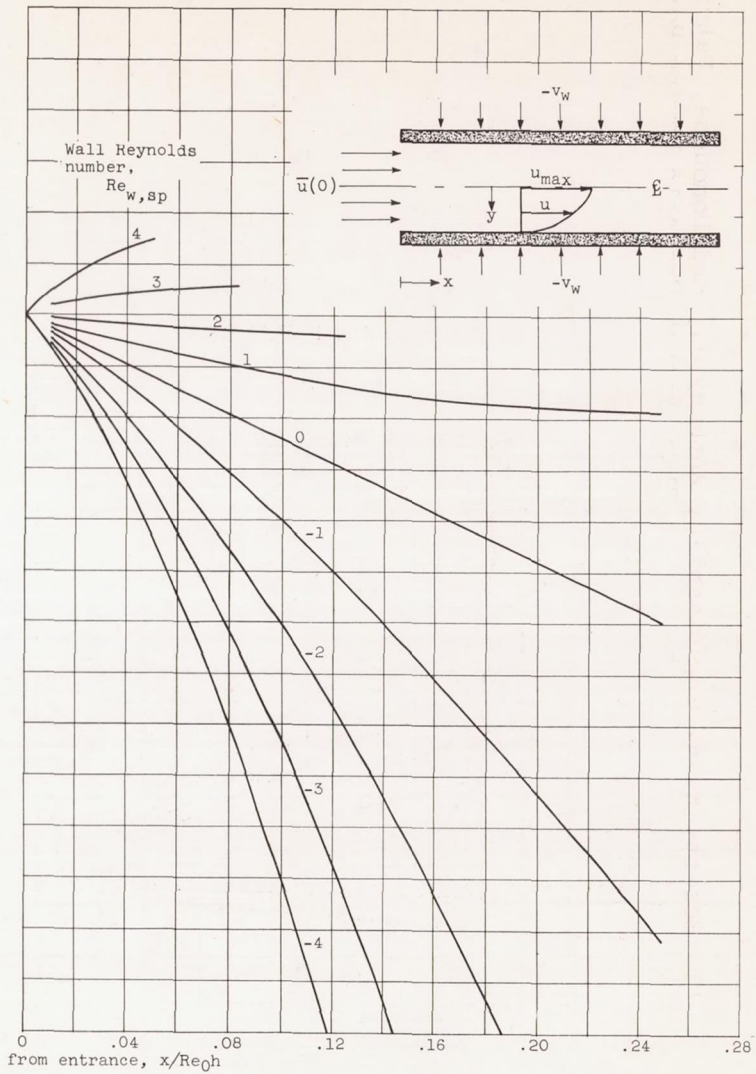Figure 2. - Concluded. Velocity distribution in porous channels.

(a) Semiporous channel.

(b) Fully porous channel.

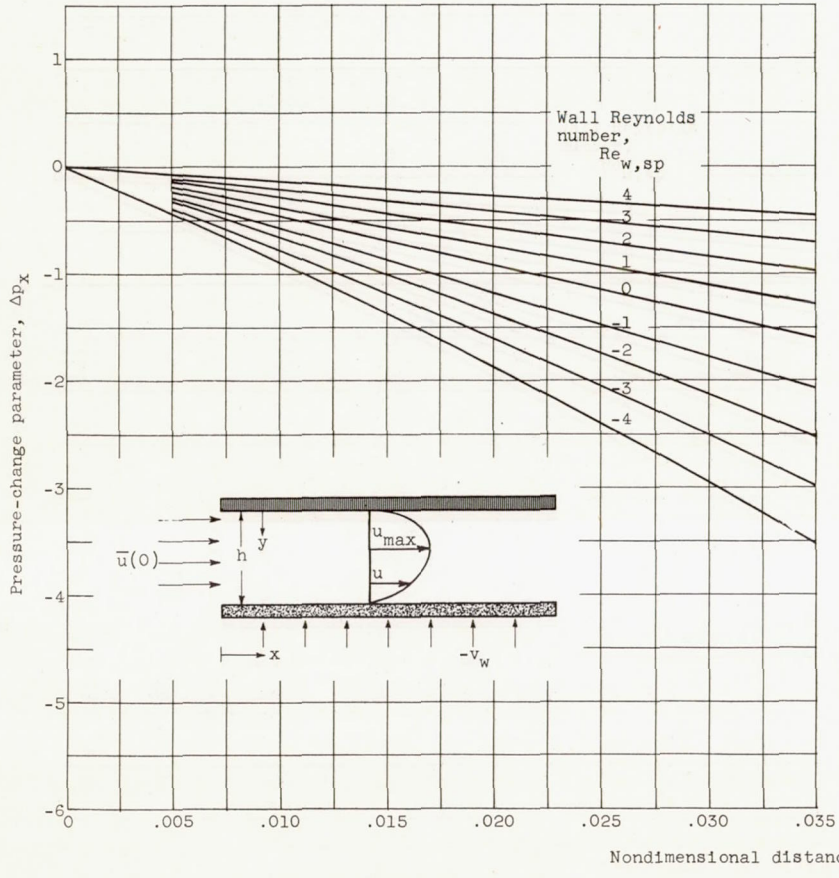Figure 3. - Pressure change in y-direction for porous channels.
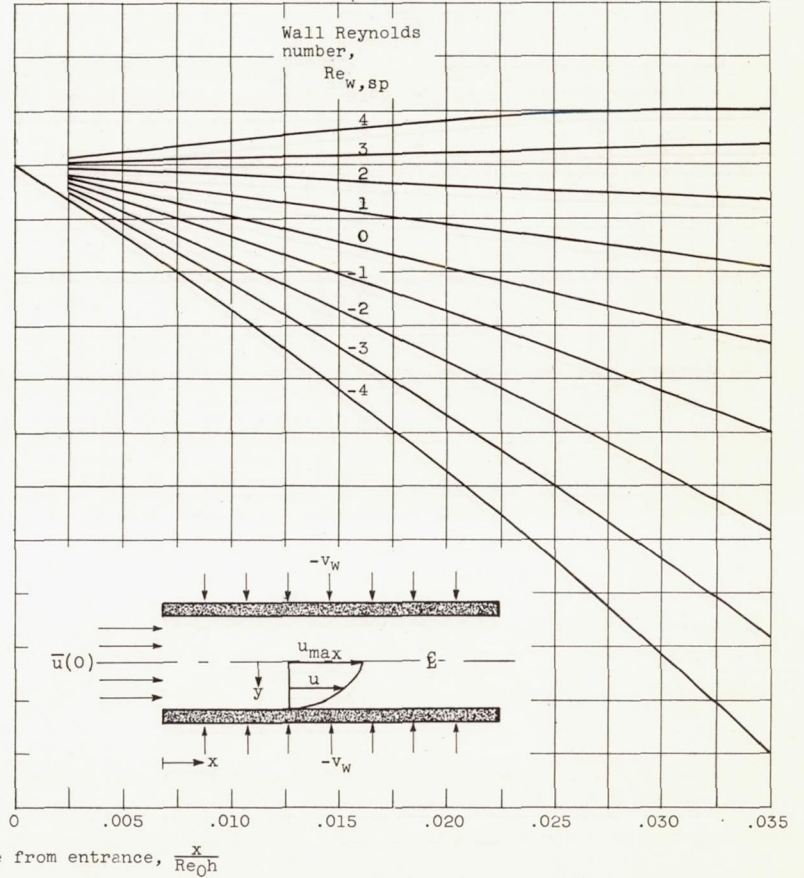
(a) Semiporous channel.　　　　　　　　(b) Fully porous channel.

Figure 4. - Pressure change in porous channels; $0 \leq \frac{x}{Re_0 h} \leq 0.25$.

(a) Semiporous channel.

(b) Fully porous channel.

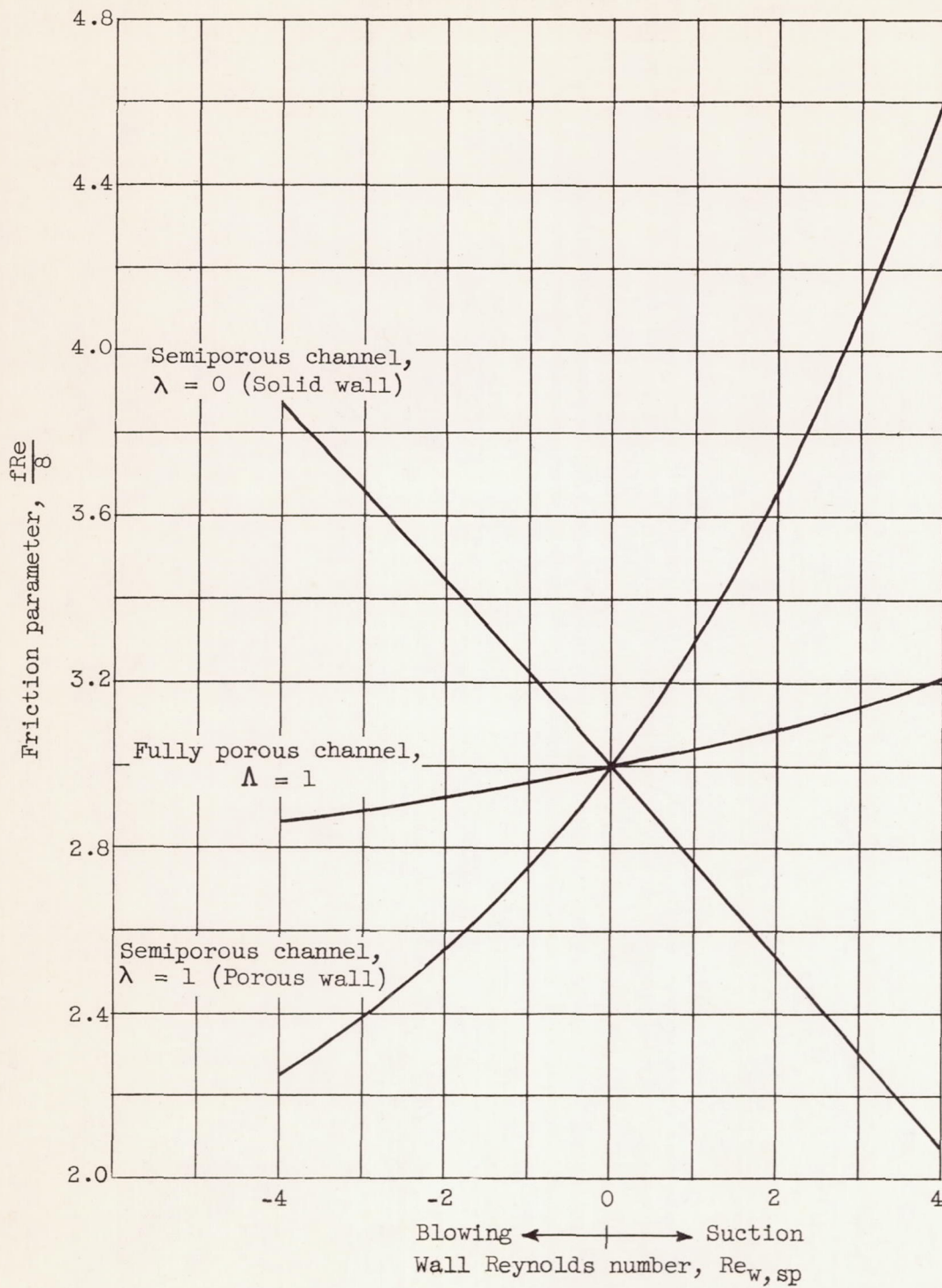Figure 5. – Pressure change in main-flow direction for porous channels; $0 \leq \frac{x}{Re_0 h} \leq 0.035$.

4056

Figure 6. - Effects of wall friction on porous channels;
$-4 \leq Re_{w,sp} \leq 4$.